

## SOME THERMAL CHARACTERISTICS OF A MINERAL MIXTURE OF PALYGORSKITE, METAHALLOYSITE, MAGNESITE AND DOLOMITE

H. Bayram<sup>1</sup>, M. Önal<sup>2\*</sup>, G. Üstünişik<sup>3</sup> and Y. Sarıkaya<sup>2</sup>

<sup>1</sup>Marmara University, Atatürk Faculty on Education, Göztepe, İstanbul, Turkey

<sup>2</sup>Ankara University, Faculty of Science, Department of Chemistry, Tandoğan, 06100 Ankara, Turkey

<sup>3</sup>University of Cincinnati, Department of Geology, Cincinnati, Ohio, USA

An industrial raw material taken from Sivrihisar (Eskişehir, Turkey) region was heat-treated at different temperatures in the range of 100–1000°C for 2 h. The volumetric percentage of the particles having a diameter below 2 µm after staying in an aqueous suspension of the material was determined as 67% by the particle size distribution analysis. The mineralogical composition of the material was obtained as mass% of 32% palygorskite, 10% metahalloysite, 35% magnesite, 20% dolomite and 3% interparticle water by using the acid treatment, X-ray diffraction and thermal analysis (TG, DTA) data.

The temperature ranges were determined for the endothermic dehydrations for the interparticle water as 25–140°C, for the zeolitic water as 140–320°C, and for the bound water as 320–480°C, in the palygorskite. The temperature range for the endothermic dehydroxylation and exothermic recrystallization of the palygorskite is 780–840°C. The temperature range for the endothermic dehydroxylation of the metahalloysite and calcinations of magnesite are coincided at 480–600°C. Dolomite calcined in the temperature range of 600–1000°C by two steps. The zig-zag changes in the specific surface area ( $S/m^2 g^{-1}$ ) and specific micro and mesopore volume ( $V/cm^3 g^{-1}$ ) as the temperature increases were discussed according to the dehydrations in the palygorskite, dehydroxylation of palygorskite and metahalloysite, and calcinations in magnesite and dolomite.

**Keywords:** dehydration, dehydroxylation, metahalloysite, palygorskite, thermal analysis, XRD

### Introduction

In general, an industrial raw material is a mixture of minerals [1]. The application areas of the raw material were determined according to their chemical and mineralogical compositions [2]. Monomineralic materials are seldom found in the nature [3]. Clays, used over hundred areas, are among the most important industrial raw materials [4–6]. Many clays are the mixture of the clay and nonclay minerals [7]. One or more clay and nonclay minerals can be found in any clay [8–11].

The clays with the major clay mineral palygorskite or sepiolite include generally carbonates such as magnesite ( $MgCO_3$ ), calcite ( $CaCO_3$ ) and dolomite ( $MgCO_3, CaCO_3$ ) as nonclay minerals [12]. Fibrous and other types of clay minerals are seldom found together in the clays. For example, few clays contain palygorskite and metahalloysite together as fibrous and layer types of clay minerals, respectively.

Several structural models for palygorskite (attapulgitite) have been discussed in [13–19]. The theoretical half unit-cell formula of palygorskite is given as  $Si_8O_{20}Mg_5(OH)_2(OH_2)_4 \cdot 4H_2O$  [20]. Palygorskite is 2:1 type phyllosilicate and derived from talc-like tetrahedral-octahedral-tetrahedral (T–O–T) ribbons, expanded infinitely along the z-direction of the fibrous

crystal, with a width of two pyroxene chains. The  $8Si^{4+}$  and  $5Mg^{2+}$  cations are located at the tetrahedral and octahedral positions of each ribbon. Some of the  $Mg^{2+}$  cations are replaced principally by  $Al^{3+}$  and  $Fe^{3+}$  cations. Palygorskite has di- or trioctahedral character depending on the divalent/trivalent cation ratio, distribution of cations, and occupancy of the octahedral sites [21, 22]. Two hydroxyls are bonded to the third  $Mg^{2+}$  among the  $5Mg^{2+}$  cations of each palygorskite ribbon. The ribbons are connected to each other by Si–O–Si bridges by each four corners to form continuous tetrahedral sheets and discontinuous octahedral sheets. The discontinuity of the octahedral sheets allows to form of rectangular channel-like nanopores with the cross-section of 0.37–0.64 nm.

Four water molecules are bonded two per two to the first and the fifth  $Mg^{2+}$  cations at the both ends of each ribbon and located in nanochannels. These molecules are called bound (structural or crystal) water in palygorskite [23]. Furthermore, four water molecules per half-unit cell are located two per two with in the nanochannels in the both side of each other ribbon. These water molecules in hydrogen bonded with bound water and each other are called zeolitic water. One water molecule per half-unit cell of palygorskite formed from two hydroxyls on the third  $Mg^{2+}$  cation

\* Author for correspondence: onal@science.ankara.edu.tr

is called dehydroxylation water. The theoretical content of the zeolitic water (ZW), bound water (BW), and dehydroxylation water (DW) in the palygorskite are calculated stoichiometrically in mass% of 8.53, 8.53 and 2.13%, respectively. The molar and mass ratios of ZW:BW:DW=4:4:1 must be constant according to the proportion law in chemistry. The moisture water located interparticle is exchangeable and not shown in the chemical formula of palygorskite.

Halloysite is a kaolin polytype which is often tubular or spherical instead of being platy [24–27]. The ideal chemical formula of halloysite is  $\text{Al}_2\text{Si}_2\text{O}_5(\text{OH})_4 \cdot n\text{H}_2\text{O}$ . The open structure of 1.0 nm halloysite allows intercalation of  $n\text{H}_2\text{O}$  molecules [28]. After dehydration of the intercalated water at about 180°C, collapsing of halloysite layers from 1.0 to 0.7 nm occurs [29–33]. Halloysite occurring without intercalated water molecules is called metahalloysite (MH). The structure of metahalloysite is more disordered than the structure of halloysite [34].

The aim of this study is the examination of thermal behaviour of a mineral mixture of palygorskite, metahalloysite, magnesite, and dolomite by using particle size, chemical, X-ray diffraction, thermal and nitrogen adsorption analyses.

## Experimental

An industrial raw material taken from Sivrihisar (Eskişehir/Turkey) region was examined in this study. The natural rock was suspended in water by stirring time to time and was held for 24 h at room temperature to obtain fine particles without any destruction. The volumetric particle size distribution (PSD) of the suspended samples after 10 min and 24 h were determined by using a Mastersizer Instrument (Malvern, Micron Model, UK). The precipitate in the suspension after staying 24 h was separated by a centrifuge (Rotofix 32, Typ 1205, Hettic), air dried, ground gently, and stored in a plastic bottle to use next experiments.

A sample of 10 g taken air dried material was heated at 100°C for 2 h in an oven (Binder, IP 20) and its moisture was determined by weighing. The rest of this sample was calcined at 1000°C for 2 h in a furnace (Alser, Protherm, PLF 12077) and its loss on ignition (LOI) was determined by weighing. For the chemical analysis, approximately 0.25 g calcined sample was weighed and put in a platinum crucible. The mixture obtained after addition of 3 g  $\text{LiB}_4\text{O}_7$  (Merck) in this sample was digested at 1000°C for 1 h and cooled to the room temperature. The crucible was inserted in a beaker of 100 mL HCl 10% solution. The system was heated at 90°C by stirring until the precipitate in the crucible was solved. The solution was di-

luted to 250 mL in a volumetric flask. The chemical analysis was determined by Hitachi Z-8200 Atomic Absorption Spectrophotometer. The results were calculated as the mass% of the metal oxides.

Thermal gravimetric analyses (TG) and differential thermal analyses (DTA) curves of the air dried sample were recorded using a Shimadzu Apparatus (DTG-60H). Approximately 20 mg of a sample was placed in a platinum crucible on the pan of the microbalance and heated in the range 25–1000°C using  $\alpha\text{-Al}_2\text{O}_3$  as inert material. Analysis was performed under flowing nitrogen with the rate of 100 mL  $\text{min}^{-1}$  and a heating rate of 10°C  $\text{min}^{-1}$ .

The air dried samples, each having a mass of 10 g, were heated in 100°C intervals up to 1000°C and were thermally treated by maintaining at each temperature for 2 h by using a furnace (Alser, Protherm, PLF 12077).

The X-ray diffraction (XRD) patterns of the natural and heat-treated samples were obtained from random mounts using a Rikagu D-Max 2200 Powder Diffractometer with  $\text{CuK}_\alpha$  radiation and a Ni filter.

To separate clay minerals from carbonate rocks in the natural material, an acid treatment was conducted. After mixing, 1.2243 g material was dried at 100°C for 2 h and a sodium acetate-acetic acid solution buffer at pH=5, 0.1 N hydrochloric acid solution was added drop by drop in the mixture until the disappearing of the carbon dioxide bubbles. The precipitate was separated, washed until being free of chloride and acetate ions, and dried at room temperature. The mass of the dried sample at 100°C for 2 h was weighed as 0.5795 g. The difference of two masses gives a total mass of the carbonates found in the sample before the acid treatment.

The adsorption and desorption of  $\text{N}_2$  at liquid  $\text{N}_2$  temperature for the natural and heated samples were determined by a volumetric adsorption instrument, of Pyrex glass, which was connected to high vacuum [35].

## Results and discussion

### Particle size analysis

The PSDs of the material held in aqueous suspension for 10 min and 24 h are shown in Fig. 1, as volumetric percentages vs. particle diameter (Vol.%– $D$ ) curve and its derivative  $[d(\text{Vol.}\%)/dD-D]$  curve. The volumetric percentages of the particles having  $D$  below 2  $\mu\text{m}$  for the samples held in aqueous suspensions for 10 min and 24 h are read from Fig. 1 as 13 and 67%, respectively. Also, their outer surface areas are measured by PSD measurements as 2.5 and 6.3  $\text{m}^2 \text{g}^{-1}$  respectively. The exact distribution of clay mineral particles below 2  $\mu\text{m}$  in water takes long time such as

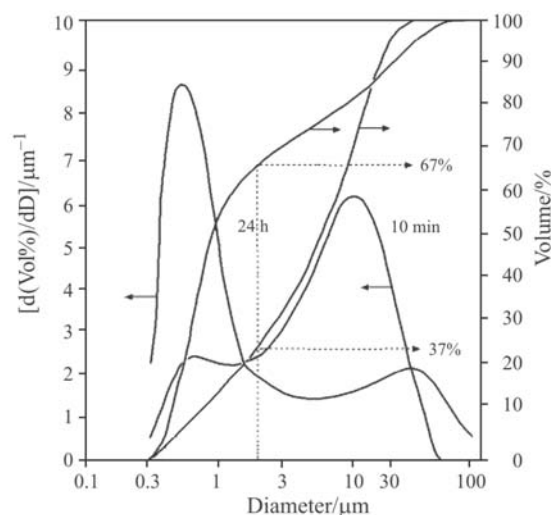


Fig. 1 Particle size distribution curves of the natural rock staying in its aqueous suspension for 10 min and 24 h

24 h. Particle sizes of nonclay minerals in water are generally larger than 2  $\mu\text{m}$ . Clay minerals can be separated easily from nonclay minerals based on the PSDs in aqueous suspensions.

#### XRD analysis

The XRD patterns are obtained from random mount of the natural rock and its heated samples are represented in Fig. 2. In the XRD patterns of the natural rock, four sharp strong reflections at 1.050, 0.644, 0.289 and 0.275 nm are due to the palygorskite (P), metahalloysite (MH), dolomite (D), and magnesite (M) [11]. The other small reflections belong to palygorskite and metahalloysite. Therefore the natural rock contains palygorskite and metahalloysite as clay minerals, and also magnesite and dolomite as nonclay minerals.

There is not any significant change in the XRD patterns of the heated samples up to 400°C as seen in Fig. 2. However, the small decrease in intensity and increase in the width of the reflection at 1.050 nm show that a little reversible folding in palygorskite structure and its nanochannels by heating up to 400°C.

The loss of reflections at 1.050 and 0.741 nm shows an irreversible folding of sepiolite and metahalloysite structures, while the heating temperature reaches to 500 and 600°C, respectively [28]. Absence of reflection at 0.275 nm shows exactly the calcinations (decarbonation) of magnesite up to 600°C. The reflections at 0.334 and 0.289 nm show the formation of quartz (Q) and calcite (C) respectively as the temperature rises to 600°C. Calcite originates from the first step calcination of dolomite. The second step calcination of dolomite is the calcination of the previously formed calcite completed exactly up to 1000°C.

New reflections show the formation of new phases in the range of 800–1000°C. The reflection at 0.398 nm

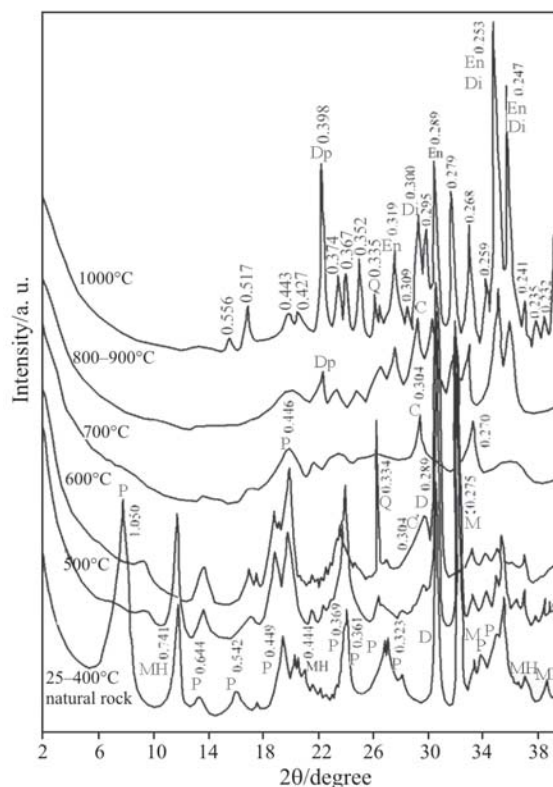


Fig. 2 X-ray diffraction patterns of the natural rock and its heat treated samples at different temperatures in the range 100–1000°C (P: palygorskite, MH: metahalloysite, D: dolomite, M: magnesite, C: calcite, Q: quartz, Dp: diasporite, En: enstatite, Di: diopside)

shows the formation of diasporite (Dp= $\alpha$ -AlOOH) originated from the recrystallization of metahalloysite. Many other reflections seen in the XRD pattern for the heated sample at 1000°C indicate the formation of enstatite (En) and diopside (Di) phases [36, 37]. The chemical formulas of the enstatite and diopside are  $\text{Mg}_2\text{Si}_2\text{O}_6$  and  $\text{CaMgSi}_2\text{O}_6$ , respectively. They have been formed by the recrystallization of the mineral mixtures, at elevated temperatures.

#### Chemical analysis

The bulk chemical analysis of the natural rock (mass%) is:  $\text{SiO}_2$ , 30.36;  $\text{Al}_2\text{O}_3$ , 1.17;  $\text{Fe}_2\text{O}_3$ , 5.49;  $\text{MgO}$ , 29.39;  $\text{CaO}$ , 4.75;  $\text{Na}_2\text{O}$ , 0.02;  $\text{K}_2\text{O}$ , 0.08, and loss on ignition (LOI) is 28.71. The  $\text{SiO}_2$ ,  $\text{Al}_2\text{O}_3$ ,  $\text{Fe}_2\text{O}_3$  and one part of  $\text{MgO}$  contents are originated from palygorskite and metahalloysite minerals. The rest of the  $\text{MgO}$  content is due to the magnesite and dolomite. The  $\text{CaO}$  content comes only from dolomite. LOI is due to the dehydration and dehydroxylation of the palygorskite, dehydroxylation of metahalloysite and calcinations of magnesite and dolomite.

There are many isomorphous substitutions among the cations in the palygorskite [21]. The  $\text{Al}^{3+}$ ,  $\text{Fe}^{3+}$  and  $\text{Fe}^{2+}$  for  $\text{Mg}^{2+}$  substitutions in octahedral chains and also

$\text{Al}^{3+}$  for  $\text{Si}^{4+}$  substitutions in tetrahedral chains of the palygorskite may occur. Positive and negative charges arising octahedral and tetrahedral replacement respectively can be largely balanced with each other. Unbalanced excess negative charge is compensated by vacancies, with one vacancy per two trivalent cations or exchangeable cations adsorbed on palygorskite crystal [22]. The divalent/trivalent cation ratio depends on the origin of palygorskite affects to some physicochemical behavior such as acid leaching and thermal treatment [38]. Since the formation of the  $\text{Fe}_2\text{O}_3$  while the heating temperature rising  $1000^\circ\text{C}$ , the gray color of the natural rock is converted to dark brown.

### Thermal analysis

Thermal analysis in combination with other techniques such as particle size, X-ray diffraction, and chemical analyses is suitable for the quantitative determination of minerals in solid mixtures [39–44]. The TG and DTA curves of the natural rock are given in Fig. 3 for the temperature range of  $25\text{--}1000^\circ\text{C}$ . Six endothermic changes and one exothermic change are seen in the DTA curve. The temperature ranges and maximum rate temperature of these changes are shown on the TG and DTA curves in Fig. 3. The changes are evaluated as below [19, 45].

The first endothermic mass loss of 3.1% between  $25\text{--}140^\circ\text{C}$  with a maximum rate at  $94^\circ\text{C}$  is due to the dehydration of interparticle water (W) or adsorbed water known also as moisture.

The second endothermic mass loss of 3.0% between  $140\text{--}320^\circ\text{C}$  with a maximum rate at  $244^\circ\text{C}$  is due to the dehydration of the zeolitic water (ZW). This mass loss must be less than or equal to the theoretical value. Other than this, a part of moisture is mistaken as zeolitic water.

The third endothermic mass loss of 3.0% between  $320\text{--}480^\circ\text{C}$  with a maximum rate at  $329^\circ\text{C}$  is due to the dehydration of the bound water (BW). Bound water molecules are lost in two steps accompanied by reversible structural change similar to sepiolite [23, 46, 47]. The loss about one half of the bound water by the first dehydration step is partially folded the nanochannels. Since the hindrance of these folded channel on the diffusion of the rest bound water molecules by second step causes a decrease in rate and consequently an increase in temperature of the dehydration. The mass losses originated from zeolitic and bound water must be equal to the percentages according to the chemical formula of palygorskite. The mass loss content for bound water must be less than or equal to the theoretical value of 8.53%. Other than this, a part of the zeolitic water is mistaken as bound water. The phase formed after the reversible dehydra-

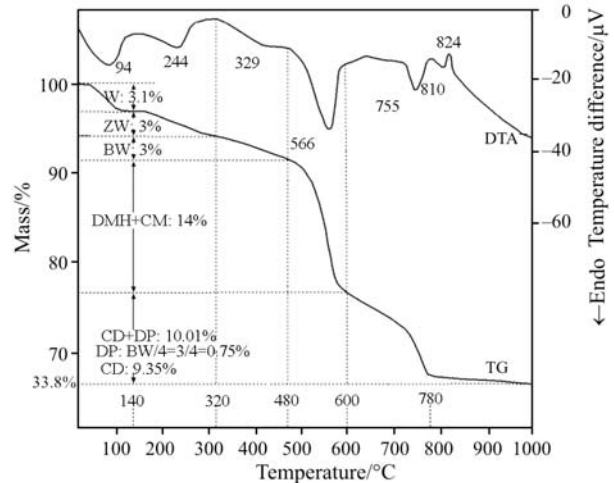
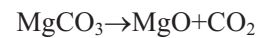


**Fig. 3** TG and DTA curves of the natural rock in the temperature range  $25\text{--}1000^\circ\text{C}$

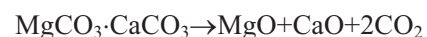
tion of bound water is called palygorskite anhydride with a chemical formula of  $\text{Si}_8\text{O}_{20}\text{Mg}_5(\text{OH})_2$ .

The fourth endothermic mass loss of 14.0% between  $480\text{--}600^\circ\text{C}$  with a maximum rate at  $566^\circ\text{C}$  is originated from the dehydroxylation of metahalloysite (DMH) and the calcination of magnesite (CM). The reactions can be represented respectively as below:



The mass losses came from metahalloysite and magnesite in the same temperature range can not be easily distinguished.

The fifth mass loss of 10.1% between  $600\text{--}1000^\circ\text{C}$  is due to a maximum rate at 755 and  $810^\circ\text{C}$  are originated from the calcination of dolomite (CD) and dehydroxylation of palygorskite (DW) to give enstatite respectively. The reactions can be represented respectively as below:



Since the ratio of  $\text{DW}/\text{BW}=1/4$  according to the chemical formula of palygorskite the mass loss by dehydroxylation must be  $3/4=75\%$ . The rest of the mass loss between  $600\text{--}1000^\circ\text{C}$  such as  $10.1-0.75=9.35\%$  is occurred by the calcination of dolomite. There is not any mass loss during the exothermic recrystallization of palygorskite and halloysite above  $800^\circ\text{C}$ . Diopside forms according to the reaction:



The phase of  $\text{Al}_2\text{O}_3$  remained from the metahalloysite is diasporite as represented in Fig. 2.

### Mineralogical analysis

The mineral content in the natural rock can be determined by using acid treatment, XRD, TG and DTA data as follows. The mass% of moisture in the natural rock is observed from TG curve as 3.1%. The mass% of sepiolite is calculated from the ratio of the bound water content in the rock to its theoretical content as  $(3.00/8.53) \cdot 100 = 35.2\%$ . The total mass% of magnesite and dolomite is calculated as  $(1.2243 - 0.5795) \cdot 1000 / 1.2243 = 52.7\%$  from the calcination data obtained by acid treatment. The dolomite percentage is calculated stoichiometrically according to the constant proportions law in chemistry as  $(184.392/88) \cdot 9.35 \cdot 100 = 19.6\%$ . Here  $184.392 \text{ g mol}^{-1}$  is the molar mass of dolomite and  $2 \cdot 44 = 88 \text{ g}$  represent the mass of carbon dioxide found in one mole of dolomite. The rest of the total mass loss after acid treatment gives the mass% of magnesite as  $52.7 - 19.6 = 33.1\%$ . The mass% of metahalloysite is the rest of 100% and calculated as  $100 - (3.1 + 35.2 + 33.1 + 19.6) = 9.0\%$ . The composition of the mineral mixture can be given approximately as 3% moisture, 35% palygorskite, 9% metahalloysite, 33% magnesite and 20% dolomite.

### Nitrogen adsorption-desorption analysis

The specific surface areas ( $S/\text{m}^2 \text{ g}^{-1}$ ) of the natural rock and heated samples were determined by the Brunauer, Emmett and Teller (BET) method by using the adsorption data [48]. The specific micro- and mesopore volumes ( $V/\text{cm}^3 \text{ g}^{-1}$ ) of same samples were calculated from the adsorption capacity as liquid nitrogen volume obtained from desorption isotherm at the relative equilibrium pressure  $p/p_0 = 0.96$  [49, 50]. The 'zig-zag' changes in  $S$  and  $V$  by the heating temperature are given in Fig. 4. The values of  $S$  and  $V$  for

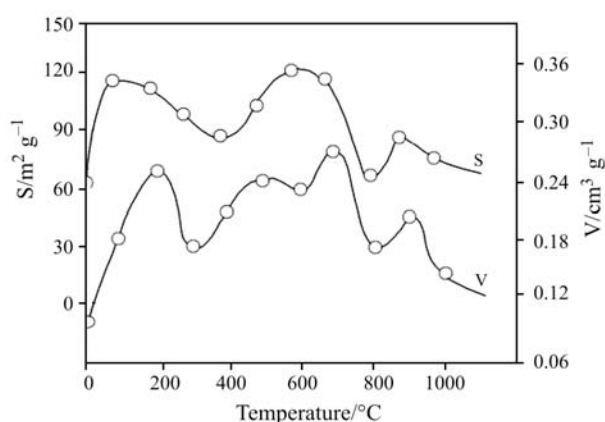


**Fig. 4** Variation of specific surface area ( $S/\text{m}^2 \text{ g}^{-1}$ ) and specific micro- and mesopore volume ( $V/\text{cm}^3 \text{ g}^{-1}$ ) of the mixture of palygorskite, metahalloysite, magnesite and dolomite by rising temperature

the natural rock are  $63 \text{ m}^2 \text{ g}^{-1}$  and  $0.10 \text{ cm}^3 \text{ g}^{-1}$ , respectively. While the temperature increases at around 200 and  $700^\circ\text{C}$  the  $S$  and  $V$  increase to their maximum values of approximately  $120 \text{ m}^2 \text{ g}^{-1}$  and  $0.26 \text{ cm}^3 \text{ g}^{-1}$  respectively. The increases are originated from the dehydration of interparticle, zeolitic and bound water of palygorskite, dehydroxylation of metahalloysite, and calcination of magnesite.

### Conclusions

Mineralogical composition of a raw material can be determined by using acid treatment, XRD, TG and DTA data. The mass% of the interparticle, zeolitic, bound and dehydroxylation water in the palygorskite were determined by thermal analysis. The content of zeolitic and bound water in palygorskite is same and must be constant according to the chemical formula. Their value in a mineral mixture is always less than the theoretical values calculated from the formula of palygorskite. The palygorskite content in a mineral mixture can be calculated from the ratio of the bound water content to the its theoretical values 8.53%.

### Acknowledgements

The authors thank the Scientific and Technical Research Council of Turkey (Tübitak) which funded this research under a Project No: TBAG-2363 (100T138).

### References

- 1 A. M. Evans, *Ore Geology and Industrial Minerals: An Introduction*, Blackwell Science, 3<sup>rd</sup> Edition, 1992.
- 2 P. A. Ciullo, *Industrial Minerals and Their Uses*, William Andrew Publishing, New York 1996.
- 3 D. A. C. Manning, *Introduction to Industrial Minerals*, Chapman and Hall, Atlanta, USA 1994.
- 4 H. H. Murray, *Appl. Clay Sci.*, 5 (1991) 379.
- 5 H. H. Murray, *Clay Miner.*, 34 (1999) 39.
- 6 H. H. Murray, *Appl. Clay Sci.*, 17 (2000) 207.
- 7 W. Petruk, *Applied Mineralogy in the Mining Industry*, Elsevier Science, Ottawa 2000.
- 8 R. E. Grim, *Applied Clay Mineralogy*, McGraw-Hill, New York 1962.
- 9 R. E. Grim, *Clays Clay Miner.*, 36 (1988) 97.
- 10 R. E. Grim and N. Güven, *Bentonites, Geology, Mineralogy, Properties and Uses, Development in Sedimentology*, Vol. 24, Elsevier, Amsterdam 1978.
- 11 D. M. Moore and R. C. Reynolds Jr., *X-ray Diffraction and the Identification and Analysis of Clay Minerals*, Oxford University Press, Oxford 1997.
- 12 R. J. Reeder, *Carbonates: Mineralogy and Chemistry: Reviews in Mineralogy*, Vol. 11, Mineralogical Society of America, Washington D.C. 1983.

- 13 W. F. Bradley, *Am. Mineral.*, 25 (1940) 405.
- 14 C. L. Christ, J. C. Hathaway, P. B. Hostetler and A. O. Shepard, *Am. Mineral.*, 54 (1969) 198.
- 15 V. A. Drist and G. V. Sokolova, *Sov. Phys. Cryst.*, 16 (1971) 183.
- 16 C. Serna, G. E. VanScoyoc and J. L. Ahlrichs, *Am. Mineral.*, 62 (1977) 784.
- 17 G. E. VanScoyoc, C. J. Serna and J. L. Ahlrichs, *Am. Mineral.*, 64 (1979) 215.
- 18 J. E. Chisholm, *Can. Mineral.*, 30 (1992) 61.
- 19 W. Kuang, G. A. Facey and C. Detellier, *Clays Clay Miner.*, 5 (2004) 635.
- 20 E. Garcia-Romero, M. S. Barrios and M. A. B. Revuelta, *Clays Clay Miner.*, 52 (2004) 484.
- 21 J. L. M. Vivaldi and P. F. Hach-Ali, Palygorskites and sepiolites, Chapter 20, In R. C. Mackenzie: *Differential Thermal Analysis*, Vol. 1, 1970.
- 22 A. Chahi, S. Petit and A. Decarreau, *Clays Clay Miner.*, 50 (2002) 306.
- 23 C. Serna, J. L. Ahlrichs and J. M. Serratos, *Clays Clay Miner.*, 23 (1975) 452.
- 24 R. L. Frost and A. M. Vassallo, *Clays Clay Miner.*, 44 (1996) 635.
- 25 R. L. Frost, *Clays Clay Miner.*, 43 (1995) 191.
- 26 R. L. Frost, L. Rintoul and R. A. Eggleton, Structural aspects of hisingerite: a vibrational spectroscopic study, *Clays Our Future, Proc. Int. Clay. Conf.*, 11<sup>th</sup>, 1997, pp. 409–412.
- 27 R. L. Frost and J. Kristóf, *Clays Clay Miner.*, 45 (1997) 551.
- 28 E. Joussein, S. Petit, J. Churchman, B. Theng, D. Righi and B. Delvaux, *Clay Miner.*, 40 (2005) 383.
- 29 R. L. Frost, J. Kristóf, E. Makó and J. T. Klopogge, *Am. Mineral.*, 85 (2000) 1735.
- 30 R. L. Frost, J. Kristóf, E. Horváth and J. T. Klopogge, *J. Colloid Interface Sci.*, 226 (2000) 318.
- 31 E. Horváth, J. Kristóf, R. L. Frost, A. Rédey, V. Vágvölgyi and T. Cseh, *J. Therm. Anal. Cal.*, 71 (2003) 707.
- 32 J. T. Klopogge and R. L. Frost, *Geologica Belgica*, 2 (2000) 213.
- 33 J. Kristóf, M. Tóth, M. Gábor, P. Szabó and R. L. Frost, *J. Thermal Anal.*, 49 (1997) 1441.
- 34 P. M. Costanzo and R. F. Giese, *Clays Clay Miner.*, 33 (1985) 415.
- 35 Y. Sarıkaya and S. Aybar, *Commun. Fac. Sci. Uni. Ank.*, 24B (1978) 33.
- 36 H. Hayashi, R. Otsuka and N. Imai, *Am. Mineral.*, 53 (1969) 1613.
- 37 U. Shuali, S. Yariv, M. Steinberg, M. M. Vanmoos, G. Kahr and A. Rub, *Thermochim. Acta*, 135 (1988) 291.
- 38 A. Corma, A. Mifsud and E. Sanz, *Clay Miner.*, 22 (1987) 225.
- 39 M. Gal, *J. Thermal Anal.*, 37 (1991) 1621.
- 40 A. Acosta, I. Iglesias, M. Aineto, M. Romero and J. Ma. Rincón, *J. Therm. Anal. Cal.*, 67 (2002) 249.
- 41 H. Zou, M. Li, J. Shen and A. Auroux, *J. Therm. Anal. Cal.*, 72 (2003) 209.
- 42 A. Fodor, L. Ghizdavu, A. Suteu and A. Caraban, *J. Therm. Anal. Cal.*, 75 (2004) 153.
- 43 J. Ma. Rincón, M. Romero, A. Hidalgo and Ma. J. Liso, *J. Therm. Anal. Cal.*, 76 (2004) 903.
- 44 N. Yener, M. Önal, G. Üstünışık and Y. Sarıkaya, *J. Therm. Anal. Cal.*, OnlineFirst, DOI: 10.1007/s10973-005-7459-0.
- 45 R. L. Frost and Z. Ding, *Thermochim. Acta*, 397 (2003) 119.
- 46 T. Kiyahiro and R. Otsuka, *Thermochim. Acta*, 147 (1989) 127.
- 47 M. R. Weir, W. K. Kuang, G. A. Facey and C. Detellier, *Clays Clay Miner.*, 50 (2002) 240.
- 48 S. Brunauer, P. H. Emmett and E. Teller, *J. Am. Chem. Soc.*, 60 (1938) 308.
- 49 S. Gregg and K. S. W. Sing, *Adsorption Surface Area and Porosity*, Academic Press, London 1982.
- 50 Y. Sarıkaya, M. Önal, B. Baran and T. Alemdaroğlu, *Clays Clay Miner.*, 48 (2000) 557.

---

Received: February 27, 2006

Accepted: April 26, 2006

OnlineFirst: August 16, 2006

---

DOI: 10.1007/s10973-006-7561-y